Econ. Environ. Geol.
Vol. 28, No. 4, p. 351-367, 1995.

Major, Trace and Rare Earth Element Geochemistry, and Oxygen-Isotope Systematics of Illite/smectite in the Reindeer D-27 Well, Beaufort-Mackenzie Basin, Arctic Canada

J. Ko*, R. Hesse** and F.J. Longstaffe***

ABSTRACT: The elemental geochemistry and oxygen isotopes of illite/smectite (I/S) have been studied in relationship to the mineralogical trend in the Reindeer D-27 well, Beaufort-Mackenzie Basin. The increase in concentrations of K_2O, Rb and rare earth elements (REE), the decrease in concentrations of octahedral elements such as Mg, Ti, Sc, Zn and Zr, and the increase in concentrations of tetrahedral elements such as Be and V can be related to I/S compositions that vary systematically with depth. Layer formulae of S- and I-layers are estimated as $[Al_{1.57}Fe_{.19}Mg_{.31}Ti_{.07}][Si_{3.84}Al_{.16}]O_{10}(OH)_2$ and $[Al_{1.84}Mg_{.16}][Si_{3.33}Al_{.67}]O_{10}(OH)_2$, respectively.

The mobilization of REE appears to occur during illitization. The increase in concentrations of REE, especially La and Ce, with depth is probably linked to incorporation of ions with high valency (e.g. V^{5+}) in tetrahedral sites. The excess valency due to V is partly counter-balanced by ions with low valency (e.g. Be^{2+}) and, in turn, the local valency deficiency caused by Be^{2+} could be compensated by high-charge interlayer cations such as REE ($+3$).

$\delta^{18}O$ values of I/S range from 2.91 to 15.72‰ (SMOW), and increase with depth, contrasting to trends observed in the Gulf Coast and elsewhere. The increase in $\delta^{18}O$ of I/S results from the rapid increase in $\delta^{18}O$ of pore water that overcomes the decrease in temperature-dependent fractionation values with increasing burial depth ($\delta^{18}O_{pore\ water} > -d\Delta_{I/S\text{-}water}$; $d\delta^{18}O_{I/S} > 0$).

Calculated $\delta^{18}O$ values of pore water in equilibrium with I/S suggest that the original water was probably meteoric water. The stratification of pore water is postulated from the presence of an isotopically light interval, about 450m thick. The depth range of the isotopically light zone overlaps, but does not coincide with the interval of lowered I-content and K_2O concentrations, suggesting that oxygens may have been exchanged independently of mineralogical and geochemical reactions.

INTRODUCTION

Illite/smectite diagenesis has been one of the most interesting subjects of clay-mineralogical and diagenetic studies in the past two decades. It has been intensely studied using a wide variety of mineralogical and geochemical techniques such as X-ray diffraction (e.g. Perry and Hower, 1970), elemental geochemistry (e.g. Hower *et al.*, 1976), K-Ar, Rb-Sr and Nd-Sm geochronology (e.g. Aronson and Hower, 1976; Morton, 1985; Ohr *et al.*, 1991), O- and H-isotopes (e.g. Yeh and Savin, 1977; Yeh, 1980), and transmission electron microscopy (e.g. Lee *et al.*, 1985). However, the impression one may get at first that it is a well understood process does not stand up under close scrutiny.

The identity of illite/smectite (I/S) as a mixed-layer clay mineral has been questioned by Nadeau et al. (1984) who, based on transmission electron microscopic thickness measurements of finely dispersed mixed-layer clays, suggested that mixed-layering is an artifact of interparticle diffraction between thin particles. The ordering reaction of random I/S that has been considered an essential part of the smectite-to-illite process by conventional viewers is being disregarded by the Ostwald ripening theory (Inoue *et al.*, 1988; Eberl and Srodon, 1988; Eberl *et al.*, 1990). The understanding that the smectite-to-illite reactions in the subsurface are slow, gradual reactions that span considerable temperature and depth ranges has been challenged on the basis of datability of I/S diagenesis (Morton, 1985; Ohr *et al.*, 1991).

Some of the problems associated with currently developed hypotheses have been discussed theoretically by Ko (1992) on the basis of various disciplines of geochemistry. Mineralogical studies of I/S in the Beaufort-Mackenzie Basin based on 215 core and drill-cutting samples from 22 wells onshore and offshore appeared, in general, to agree to the conventional views (Ko and Hesse, 1995). The findings of interest will be further discussed in the relevant section of the paper. This paper

*Korea Institute of Geology, Mining and Materials
**McGill University, Montreal, Canada
***The University of Western Ontario, London, Canada

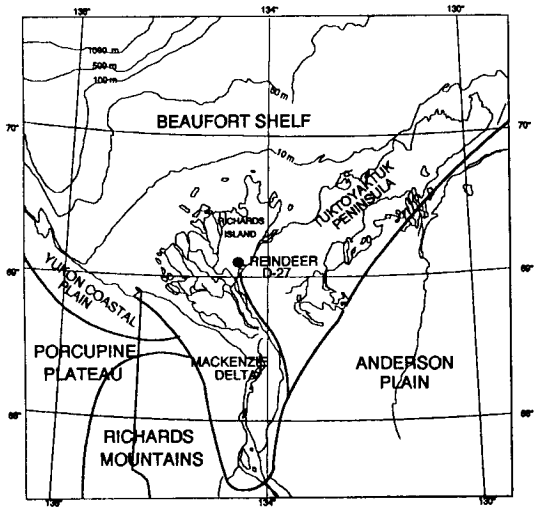

Fig. 1. Well location map.

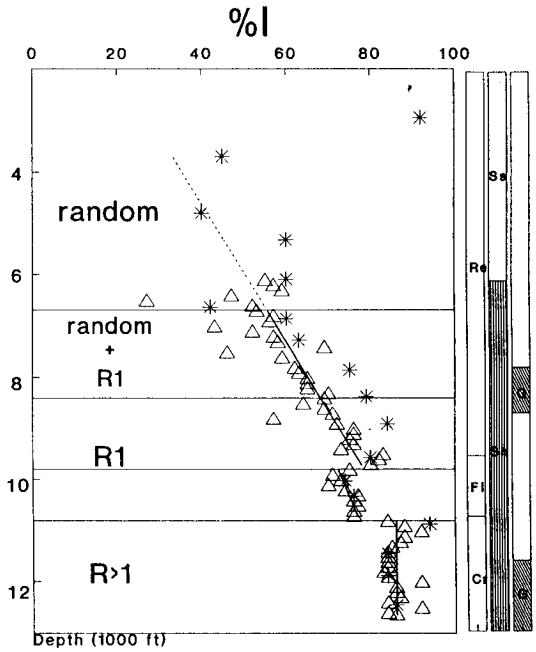

Fig. 2. Plot of I-content (%I) in I/S with respect to depth, stratigraphy, lithology, and geopressure for the Reindeer D-27 well. *- cores, Δ-drill-cuttings. Cr- Cretaceous (Albian), Fi- Fish River, Re- Reindeer. Sh- shale, Ss- sandstone, G- geopressured.

discusses the major, trace and rare earth element geochemistry, and O-isotope compositions of I/S in relation to mineralogical changes identified in the Reindeer D-27 well (Ko, 1992). Elemental geochemistry and oxygen isotopes provide information on the behavior of atoms in I/S, i.e. interlayer and structural cations, and anions, respectively, during I/S diagenesis.

WELL DESCRIPTION

B.A.-Shell-IOE Reindeer D-27 is located at the southern tip of Richards Island in the northwestern District of Mackenzie, Canada (lat. 69° 6′ 5″, long. 134° 6′ 4″; Fig. 1). It penetrated a total depth of 12668ft (3861.2 m) [The non-SI unit is used to avoid errors from rounding-off]. A bottom-hole temperature of 78.9℃ was reported.

The stratigraphic section of Reindeer D-27 comprises Lower Cretaceous (Albian) shale and Tertiary deltaic successions that include Fish River, Reindeer, Richards, Kugmallit, and Iperk sequences (Fig. 2). The Fish River Sequence consists mainly of prodeltaic shales. The Reindeer Sequence includes relatively homogeneous prodeltaic shale and overlying delta front/delta plain sandy sediment, the facies boundary of which is placed at about 6200ft (1890m). The younger sequences were not studied because of bad quality of samples. The well contains two geopressure zones: one between 7800 and 8700ft (2377~2652 m), and the other with the top at 11600ft (3536m) (Hitchon *et al.*, 1990).

Conventional core samples were available for the depth range between 2907 and 12463ft (886~3799m). Well-consolidated drill-cutting samples were available below a depth of 6100ft (1859m). Note that the stratigraphic section below 6200ft (1890m) consists predominantly of mudrocks and, thus, lithology is not considered to be a factor to influence geochemical and isotopic variations.

I/S MINERALOGY AND BURIAL TREND

I/S in Reindeer D-27 includes random, a mixture of random and ordered, R1-ordered, and R>1-ordered I/S [A mixture of random and ordered I/S shows X-ray diffraction patterns consisting of both random and R1-ordered I/S; For detailed description and discussion, see Ko and Hesse, 1995]. The proportion of I-layers increases with depth, while the dominant type of I/S changes from random to R>1-ordered I/S (Fig. 2). Random I/S, for which compositions vary from 27 to 60 %I, predominates at shallow depths above 6700 ft (2042m). Between 6700 and 8350ft (2042~2545m), a mixture of random and ordered I/S occurs, for which the relative abundance of ordered I/S increased with depth. Compositions of the mixture range from 52 to 70 %I. R1-ordered I/S is dominant in the interval between 8350 and 10800ft (2545~3292m), and contains between

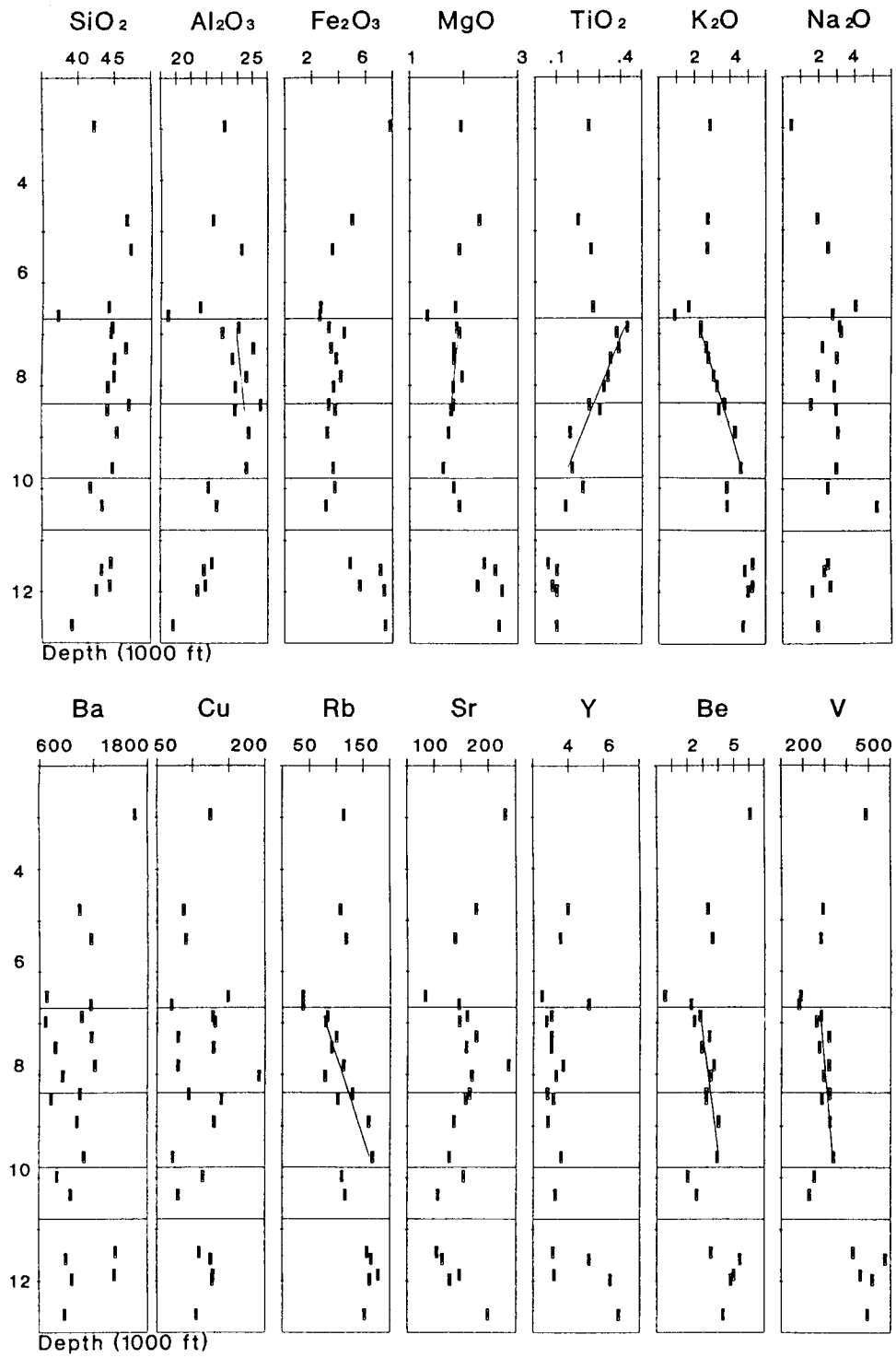

Fig. 3. Major and trace element concentrations in <.1 μmfractions of the Reindeer D-27 well with respect to depth. For major elements, the unit is wt.%; for trace elements, ppm. Horizontal lines divide the intervals based on I/S mineralogy and composition: <6700- random I/S; 6700-8350- mixture of random and ordered I/S; 8350-10800- R1-ordered I/S; 9800-10800- lowered I-content; >10800ft- R>1-orderedI/S (Cretaceous).

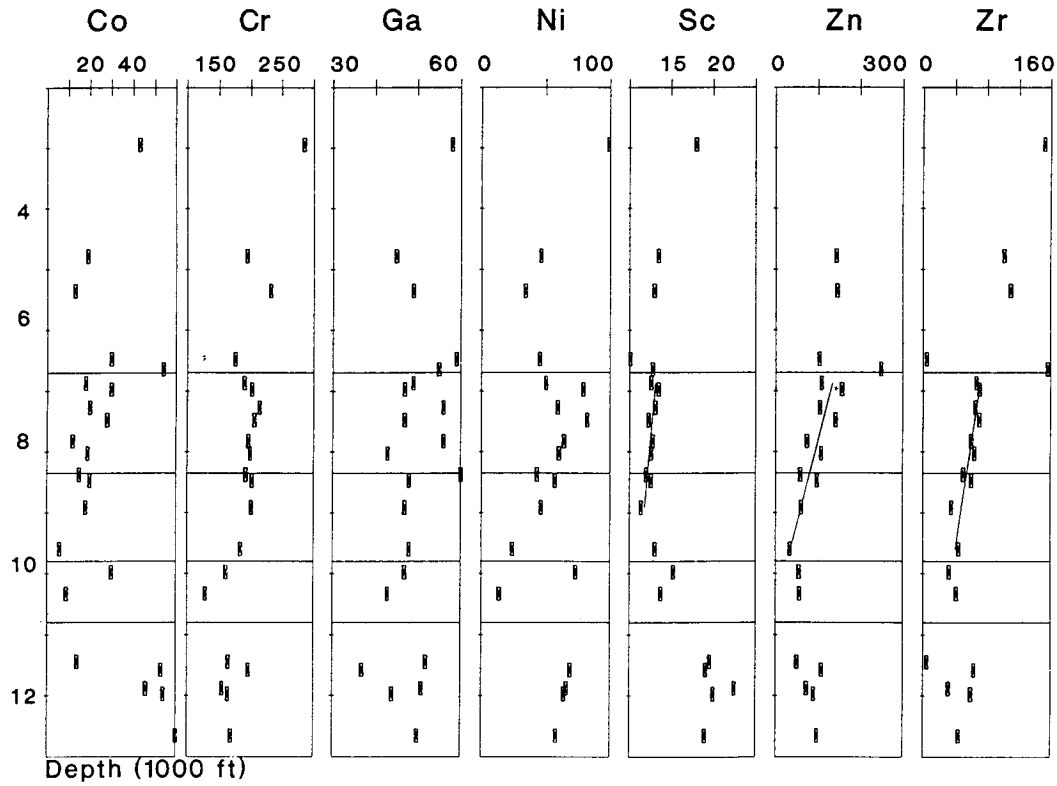

Fig. 3. continued.

69 and 80 %I. Below 10800ft (3292m), only R>1-ordered I/S with >80 %I is present.

In the interval of random I/S above 6700ft (2042m), no systematic trend was observed, though there were indications which suggest that illitization might have-taken place. Collapse of expandable layers upon K-saturation was considerable in all samples except for that from 3700ft (1128m), i.e. some expandable layers in I/S have developed high enough layer-charges to form illite-like layers if K^+ were available (Ko and Hesse, 1995).

The depth range between 6700 and 9800ft (2042~2987m) is characterized by linearly increasing I-contents with depth (1.15 %I/100ft), and consists of the intervals representing a mixture of random and ordered I/S, and R1-ordered I/S.

A noticeable discontinuity occurs between 9800 and 10800ft (2987~3292m), in which the I-content is significantly lower compared to sections above and below. The interval displays its own I/S composition gradient (0.5 %I/100ft) which is less than half of that for the stratigraphic section above.

Below 10800ft (3292m), I/S composition changes relatively little with depth. The depth coincides with the regional unconformity between the Tertiary and the Cretaceous.

SAMPLES AND EXPERIMENTAL METHODS

Samples for geochemical and isotope analyses were prepared without the chemical treatments that were applied in the mineralogical studies carried out parallel with this work (Ko and Hesse, 1995). Preliminary analyses of the mineralogical samples (<.1 μm fractions) indicated a high degree of contamination by sodium metaphosphate that was used as dispersant, despite of up to three days of dialysis. Therefore, untreated samples were size-fractionated from the same or similar subsurface depth, in cases where previous sample preparation had consumed all material. Only soluble salts were removed by dialysis until chloride was no longer detected with $AgNO_3$ solution. The <.1 μm fractions were collected by centrifugation, and freeze-dried. The <.1 μm-fraction samples contained, besides I/S, a very small amount of discrete illite and kaolinite, usually <~5% (Ko and Hesse, 1995). Chlorite appeared starting at 10800ft (3292m).

Table 1. Major and trace element concentration data. Reindeer D-27. Sample depth for drill cuttings-median depth in feet. *-core samples.

1) Major elements (wt %)

Sample depth	SiO_2	Al_2O_3	Fe_2O_3	MnO	MgO	CaO	Na_2O	K_2O	TiO_2	P_2O_5	LOI	Total
2945*	42.15	23.13	7.80	0.07	1.95	0.86	0.48	2.87	0.25	0.32	19.58	99.46
4782*	46.53	22.39	5.00	0.06	2.29	0.81	1.91	2.72	0.20	0.20	17.74	99.85
5355*	47.07	24.46	3.54	tr	0.92	0.24	2.50	2.70	0.26	0.16	16.89	99.74
6475	44.09	21.57	2.70	tr	1.85	0.35	4.04	1.67	0.27	0.26	22.94	99.74
6641*	37.14	19.46	2.62	tr	1.33	2.29	2.77	0.88	1.10	0.54	31.62	99.75
6872*	44.57	24.07	3.29	tr	1.87	0.44	3.15	2.33	0.43	0.22	19.43	99.80
6975	44.40	23.01	4.41	0.02	1.92	0.64	3.24	2.31	0.38	0.24	18.61	99.18
7270*	46.45	25.03	3.45	tr	1.82	0.34	2.22	2.62	0.39	0.20	17.13	99.65
7475	44.89	23.66	3.83	tr	1.82	0.72	3.00	2.74	0.35	0.22	18.69	99.92
7825*	44.90	24.57	4.16	tr	1.97	0.59	1.95	3.04	0.34	0.20	17.86	99.58
8025	44.07	23.85	3.62	tr	1.81	0.70	2.87	3.22	0.32	0.20	18.98	99.64
8275*	46.97	25.51	3.27	tr	1.81	0.45	1.58	3.65	0.25	0.17	15.87	99.53
8475	44.02	23.82	3.74	tr	1.77	0.72	2.97	3.32	0.30	0.20	18.86	99.72
8915*	45.37	24.73	3.16	tr	1.72	0.19	3.08	4.24	0.16	0.16	16.59	99.40
9597*	44.75	24.57	3.59	tr	1.62	0.20	3.00	4.58	0.17	0.14	16.74	99.36
9975	41.70	22.10	3.70	0.02	1.82	1.92	2.54	3.79	0.22	0.15	22.11	100.07
10329*	43.26	22.64	3.04	0.02	1.92	0.60	5.24	3.82	0.14	0.17	18.06	98.91
10975*	29.95	14.82	16.73	0.71	2.56	1.58	2.66	2.70	0.08	1.12	26.39	99.30
11443*	44.47	22.32	4.83	0.06	2.37	0.20	2.52	5.25	0.06	0.26	17.08	98.42
11575	43.21	21.81	7.08	0.30	2.58	0.64	2.33	4.83	0.10	0.30	16.47	99.65
11884*	44.37	21.91	5.55	0.39	2.25	0.29	2.66	5.25	0.08	0.17	16.65	99.57
11975	42.53	21.39	7.34	0.50	2.70	0.96	1.67	5.00	0.10	0.40	17.03	99.62
12655	39.14	19.81	7.44	0.72	2.65	1.70	1.97	4.73	0.10	0.69	20.13	99.08

2) Trace elements (ppm)

Sample depth	Ba	Be	Co	Cr	Cu	Ga	Nb	Ni	Rb	Sc	Sr	Th	V	Zn	Zr
2945*	1664	6.08	43	285	125	58	<5	99	114	18	231	15	488	443	152
4782*	1051	3.29	19	194	88	45	<5	46	108	14	177	<5	290	144	102
5355*	1172	3.59	13	232	91	49	<5	34	118	13	138	<5	280	146	110
6475	682	0.50	30	176	149	59	10	45	38	10	83	<5	188	104	5
6641*	1168	2.20	54	386	71	55	12	33	38	13	145	<5	180	249	156
6872*	1069	2.79	18	190	128	49	<5	50	83	13	160	<5	282	109	67
6975	667	2.40	30	202	131	47	5	79	80	14	146	<5	261	157	71
7270*	1176	3.40	20	214	80	56	<5	59	100	13	177	<5	319	105	66
7475	780	2.90	28	206	129	47	5	82	91	12	159	<5	273	142	71
7825*	1216	3.70	12	196	80	56	<5	64	113	13	236	<5	319	75	61
8025	854	3.50	19	199	192	43	<5	60	79	13	169	<5	294	108	65
8375*	1055	3.20	15	192	95	60	<5	43	130	12	165	<5	322	59	51
8475	736	3.20	20	202	140	48	<5	57	103	13	158	<5	287	98	61
8915*	1023	4.00	18	201	130	47	<5	46	160	11	136	<5	323	61	36
9597*	1101	3.90	6	184	73	48	<5	24	167	13	128	<5	339	35	45
9975	803	2.00	30	161	114	47	5	73	110	15	154	<5	251	56	33
10329*	952	2.58	9	129	80	43	<5	14	116	14	107	<5	228	57	42
10975	648	4.00	167	154	96	34	<5	75	114	15	285	<5	550	161	44
11443*	1444	3.50	14	165	109	52	<5	41	157	20	105	<5	427	51	5
11575	904	5.40	53	197	125	37	<5	69	165	20	115	<5	574	109	64
11884*	1430	5.00	46	155	128	51	<5	66	178	23	147	<5	461	74	32
11975	968	4.80	54	164	127	44	<5	64	162	20	129	9	515	90	60
12655	889	4.30	60	169	105	50	<5	58	152	19	198	5	492	98	45

Major, trace and rare earth element analyses were carried out by induction-coupled plasma atomic emission spectrometry [Services of the Centre de Recherches Petrographiques et Geochimiques, Centre National de

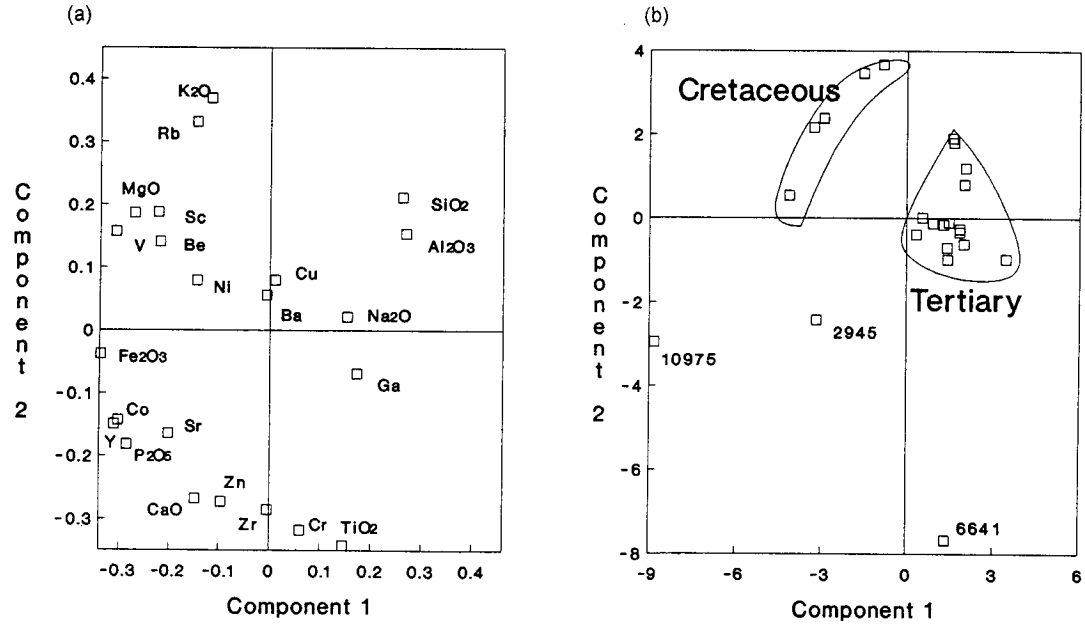

Fig. 4. Plots of principal component analysis. (a) Principal components, (b) Scatter diagram.

la Recherche Scientifique, Vandoeuvre, France] (for accuracy and precision, see Geostandard Newsletter, 1982, Vol. 6, 91-159; 1988, Vol. 12, 119-201).

O-isotope analyses (Isotopic Laboratory, Department of Geology, University of Western Ontario) were conducted according to standard procedures: pretreatment at 200℃ for 2 hours for removal of adsorbed and interlayer water; extraction of oxygen by fluorination (Clayton and Mayeda, 1963); and conversion to CO_2. Accuracy of the analyses was checked by monitoring the $\delta^{18}O$ of standard NBS-28 (9.64‰ relative to SMOW) analyzed in cycle with the samples. The mean $\delta^{18}O$ value of the NBS-28 standard was 9.72‰.

RESULTS

Geochemistry

Concentrations of major and trace elements are shown in Table 1 and plotted with respect to depth and mineralogy in Fig. 3. Fig. 4 shows the results of principal component analysis (PCA) for major and trace elements and the scatter diagram of the data with respect to the first two principal components.

PCA is efficient, as a starting point, for differentiating samples in a multivariate data set, and identifying the most effective variables, i.e. elements that could be used to characterize samples. Elements having a positive correlation plot close together (e.g. Rb-K_2O, Al_2O_3-SiO_2), whereas elements having a negative correlation plot at great distance in the diagram (e.g. K_2O-TiO_2). Elements showing least inter-sample variability plot close to the origin (e.g. Ba, Cu). The results show that Cretaceous samples are markedly different from Tertiary samples and plot in a separate field (Fig. 4b). Three samples from the depths of 2945, 6641, and 10975ft plot in isolation. Sample 2945 showed an unusually high I-content (92%I) for the shallow burial depth where most I/S is random (Fig. 2). Sample 6641 is probably bentonitic. Sample 10975 contained a considerable amount of chlorite (Ko, 1992). These samples were excluded in further data analysis and interpretation.

Major Elements

Potassium and titanium display systematic antithetic trends with depth in the interval where ordered I/S appears (6700~9800 ft; 2042~2987m): concentrations of potassium increase, whereas those of titanium decrease (Fig. 3). However, both elements do not show trends in the interval of random I/S. Concentrations of these elements are relatively uniform in the Cretaceous interval. A lower K_2O concentration is observed in the interval just above the Cretaceous section, for which mineralogical analyses indicated lowered I-contents in I/S.

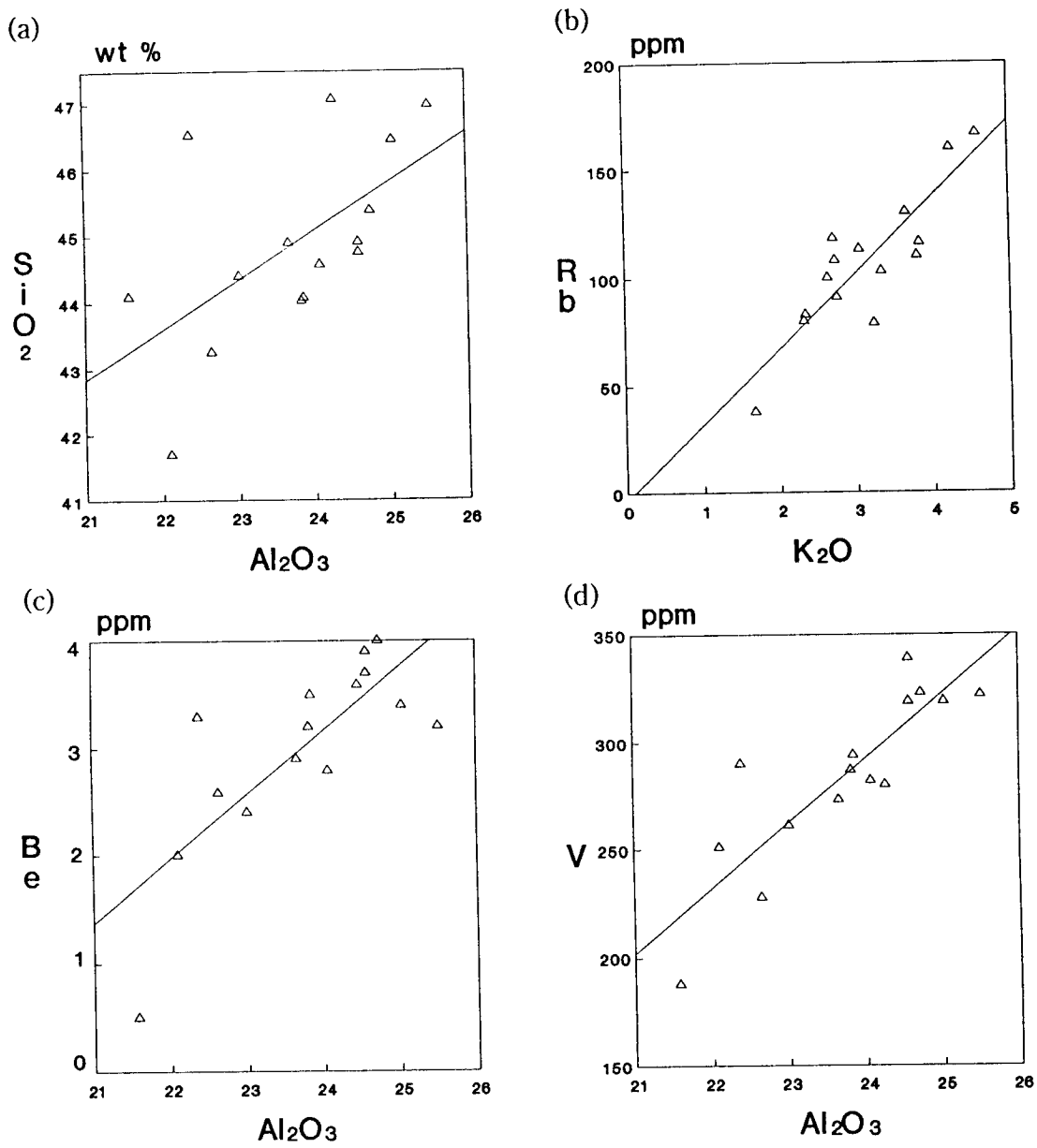

Fig. 5. Scatter plots of positively correlated elements. Cretaceous samples are not included. a) Al_2O_3-SiO_2, b) K_2O-Rb, c) Al_2O_3-Be, d) Al_2O_3-V.

Major structural, i.e. tetrahedral and octahedral, elements such as Si, Al, Feand Mg do not display clear depth-trends, however, their behavior and/or concentrations are significantly different in intervals delineated on the basis of I/S mineralogy and composition (Fig. 3). In the interval of random I/S, the data points for most elements are scattered, but some SiO_2 concentrations are higher than in other intervals. In the interval where R1-ordered I/S appeared, concentrations of Al_2O_3 seem to increase with depth, while concentrations of MgO decrease. In this interval, SiO_2 and Fe_2O_3 concentrations are more or less uniform at about 44.95% and 3.57%, respectively. The Cretaceous interval is characterized by relatively low concentrations of SiO_2 and Al_2O_3, and higher concentrations of Fe_2O_3 and MgO compared to the Tertiary section. This may be partly due to the

Table 2. Rare earth element concentration data. Unit is ppm.

Sample depth	La	Ce	Nd	Sm	Eu	Gd	Dy	Yb	Y
2945*	12.20	22.63	9.65	2.49	0.49	2.51	1.80	1.03	10.42
4782*	5.11	7.50	3.41	0.74	0.17	0.87	0.65	0.42	3.95
5355*	6.67	11.52	4.68	1.26	0.23	1.15	0.63	0.39	3.53
6475	6.01	8.39	4.75	1.13	0.26	0.80	0.79	0.26	2.48
6641*	11.85	21.04	7.25	1.70	0.28	1.25	0.97	0.44	5.14
6872*	8.29	13.38	4.80	1.20	0.20	1.10	0.64	0.35	3.02
6975	6.44	11.88	4.71	0.93	0.21	1.19	0.63	0.33	2.74
7270*	8.59	12.84	5.10	0.97	0.18	0.93	0.61	0.36	3.02
7475	7.19	12.04	4.19	1.05	0.18	0.86	0.53	0.35	3.01
7825*	12.66	22.03	6.60	1.25	0.22	1.45	0.65	0.46	3.68
8025	8.75	15.68	4.57	1.13	0.17	0.97	0.59	0.39	3.29
8375*	11.63	16.33	4.54	1.05	0.18	0.80	0.58	0.31	2.81
8475	9.60	15.10	4.62	0.95	0.19	0.72	0.58	0.36	3.14
8915*	11.23	14.41	3.77	0.90	0.15	1.00	0.48	0.33	2.84
9597*	12.68	18.44	6.32	1.36	0.21	1.21	0.66	0.48	3.59
10329*	5.66	10.82	4.12	1.20	0.15	1.32	0.67	0.35	3.24
10975	9.18	23.26	9.67	2.59	0.61	2.60	2.05	0.79	12.10
11443*	4.69	8.35	3.87	1.48	0.19	1.06	0.74	0.47	3.12
11575	6.81	13.25	4.54	0.99	0.22	1.13	0.86	0.55	5.17
11884*	5.86	10.58	4.39	1.13	0.16	0.98	0.63	0.45	3.19
11975	8.11	15.94	5.88	1.47	0.30	1.49	1.05	0.61	6.35
12655	7.91	15.55	5.72	1.24	0.28	0.86	1.14	0.61	6.82

presence of chlorite. However, core samples (11443, 12462ft) that do not contain appreciable amounts of chlorite (Ko, 1992) also show different concentrations for these elements from the Tertiary.

Interlayer cations other than K^+, i.e. Na^+ and Ca^{2+} do not show systematic depth-trends. Nonetheless, these cations were negatively correlated with SiO_2 and Al_2O_3 which are positively correlated with each other. The apparent positive correlation between Al_2O_3 and SiO_2 (Fig. 5a) is due to the presence of kaolinite in the samples. The effect of kaolinite on Al_2O_3 and SiO_2 concentrations appears greater than that resulted from differences in I-contents of I/S. The molar ratios of Al_2O_3 and SiO_2 in kaolinite do not vary significantly compared to I/S minerals. Variations in the abundance of kaolinite relative to I/S would modify the relative concentrations of Al_2O_3 and SiO_2 with respect to other elements, and result in collinearity between Al_2O_3 and SiO_2. Concentrations of Na_2O and CaO that occur exclusively in I/S of the fine clay fractions, decrease as the proportions of kaolinite increase, and vice versa.

Trace Elements

Trace elements can be grouped into 4 categories based on ionic size, coordination, valency and behavior: interlayer, tetrahedral, octahedral, and adsorbed elements. Interlayer elements include Ba, Cu, Rb, Sr and Y. These elements are characterized by large ionic radii (>.8Å) and cubic coordination. Concentrations of Rb increase more or less linearly with depth (Fig. 3), and show a positive correlation with K_2O (Fig. 5b). Concentrations of Ba, Cu, Sr and Y are variable.

Be and V, because of their relatively small ionic size, are candidates for tetrahedral occupancy. Concentrations of both elements increase with depth (Fig. 3), and show positive correlations with Al_2O_3 (Fig. 5c, d). Octahedral elements may include Co, Cr, Ga, Ni, Sc, Zn and Zr. These elements show a large difference in concentrations between Cretaceous and Tertiary intervals. The Cretaceous interval is characterized by higher Co, Sc, V, and lower Cr concentrations compared to the Tertiary interval. Concentrations of Sc, Zn and Zr decrease with depth in the Tertiary interval (Fig. 3).

Nb and Th do not show a significant relationship to depth, stratigraphy or other elements. This and very low concentrations (<5 ppm) suggest that these elements are probably not structurally bound, and may belong to the group of adsorbed elements.

Rare Earth Elements

Concentrations of rare earth elements (REE) are considerably lower than North American shale composition (NASC) and clay minerals previously studied (Cullers et al., 1975; Chaudhuri and Cullers, 1979; Clauer et al., 1990) [Table 2, Fig. 6]. However, the relative distribution of REE is similar to NASC, being enriched in light REE relative to heavy REE. La/Yb, La/Sm, Gd/Yb, and Sm/Eu ratios range between 11-38, 3-13, 2-4, 4-8, and average 18.5, 6.7, 2.6 and 5.3, respectively. Concentrations of light REE, especially La and Ce, increase with depth in the main interval of the Tertiary section (Fig. 7). Both elements show strong positive correlations to Al_2O_3, Be and V (Fig. 8). Correlations with K_2O and Rb, for which REE are supposed to substitute because of their large ionic size, though less obvious, are positive. No definite correlations with Y and Sc were detected, despite the chemical affinity of the REE to these elements.

Cretaceous samples are relatively depleted in light REE and enriched in heavy REE compared to Tertiary samples. Two samples, 2945 and 10975, which were significantly different in geochemistry and mineralogy from others, show a relatively high REE content.

Structural Formulae

Several elements showed systematic trends in the depth range from about 6700 to 9800ft (2042~2987m).

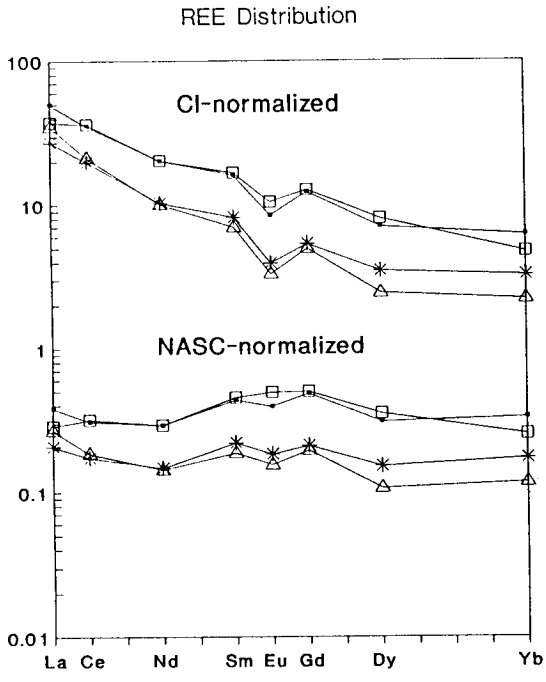

Fig. 6. Distribution of rare earth elements. CI- Chondrite I, NASC- North American Shale Composition. *; Tertiary sample average, Δ; Cretaceous sample average, ■; Sample 2945. □; Sample 10975.

Structural formulae were calculated for I/S from that interval. It was assumed (i) that the total cationic-charge equals the total layer-charge q_T, (ii) that the octahedral charge q_o equals (No. of Mg^{2+} −No. of Ti^{4+} in the formula unit) and (iii) that the tetrahedral charge equals (q_T - q_o) (Table 3). The excess and/or shortage of up to | 16 | and | 26 | for Si and Al, respectively, in the structural formula-unit were noted. These aberrations might be due to the presence of kaolinite, discrete illite (?) and probably amorphous phases (Foscolos and Powell, 1982). However, systematic corrections could not be made because of the small amounts of these impurities (e.g. <5% for kaolinite). Semi-quantitative analysis by X-ray diffraction methods has a precision >± 5% which is too large an error margin compared to the relatively small differences between samples. Discrete illite cannot be distinguished from elementary illite particles (sensu Altaner and Bethke, 1988) that were originally stacked in crystallites of I/S, but dissociate and contribute the intensity to peaks of discrete illite (Ko and Hesse, 1995). An exceptionally good alignment of K_2O data points for samples between 6475 and 9597ft (correlation coefficient: .9858) suggests that most illite was originally part of I/S. Otherwise, the concentration of potassium would vary depending on the relative abundance of discrete illite present in the samples.

Oxygen Isotopes

$\delta^{18}O$ values range from 2.91 to 15.72‰ (relative to SMOW), which are considerably lower than the Gulf Coast results of Yeh and Savin (1977). $\delta^{18}O$ values generally increase with depth. This trend is opposite to that in the Gulf Coast where $\delta^{18}O$ values decrease with depth. $\delta^{18}O$ values increase linearly and relatively rapidly in the interval of random I/S (0.20‰/100ft) (Fig. 9). Between 6700 and 10028ft (2042~3057m) the increase slows down, and the gradient flattens to about 0.03‰/100 ft. At 10329 ft (3148 m), the value abruptly falls to 11.41‰. Low values of this magnitude continue down to 11443ft (3488 m). At 11575ft (3528 m), the $\delta^{18}O$ returns to a high value of 14.54‰ below which depth little change was observed. At about the same depth (11600ft; 3536m), geophysical logs indicate the onset of geopressure in the Cretaceous section (Hitchon *et al.*, 1990).

INTERPRETATION AND DISCUSSION

Geochemistry

The differences in chemical composition, especially concentrations of several structural elements and probably REE, between Cretaceous and Tertiary samples indicate that they may not share a common provenance. Though the general source for both Cretaceous and Tertiary sediments is the Cordilleran Orogen, the mode of deposition was significantly different. Flyschoid and molassoid sedimentation in the foreland basin of the rising Cordillera dominated the Cretaceous (Albian) depositional system. As the basin became mature, the fluvio-deltaic system with its depocentre in the Beaufort-Mackenzie Basin was established in the latest Cretaceous to Early Tertiary. Although the exact provenance of the I/S mixed-layer clays is not known, higher concentrations of MgO, Fe_2O_3, most octahedral and tetrahedral trace elements, and heavy REE in the Cretaceous samples suggest less silicic parental rocks.

Several elements showed systematic trends with respect to depth. Concentrations of octahedral elements generally decrease, while concentrations of tetrahedral elements increase with depth. Concentrations of interlayer elements other than K, Rb and REE do not show a definite trend. Among the elements assigned to various sites, Cu, Ga, Sc, Y, Zn, Zr and REE require some consideration. Cu was assigned to an interlayer position,

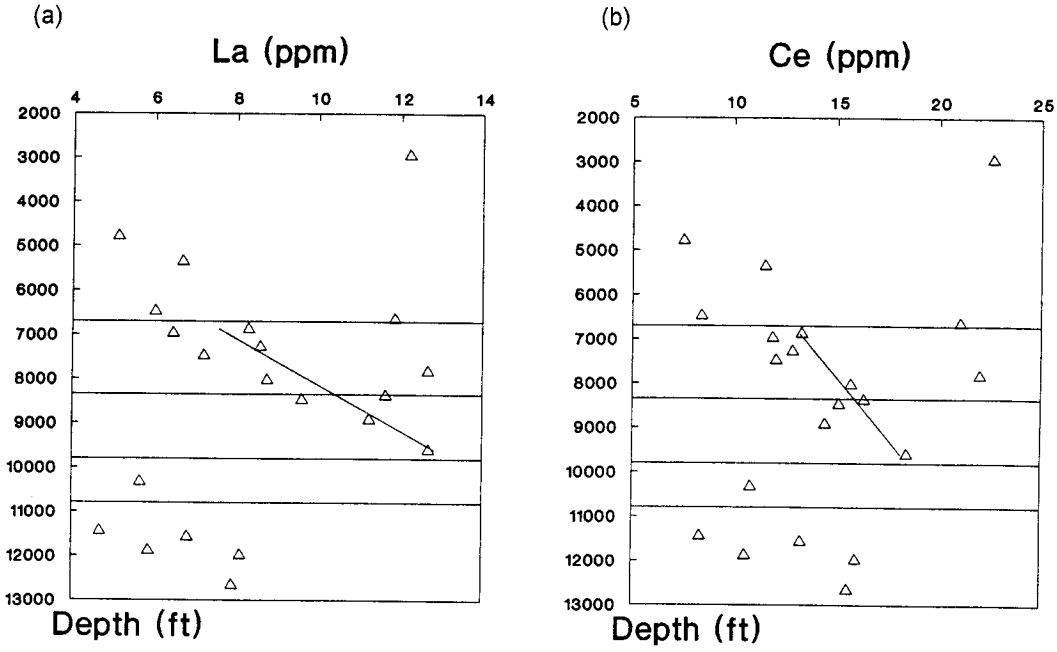

Fig. 7. La and Ce concentrations as function of depth. Horizontal lines delineate the same I/S divisions as in Fig. 3.

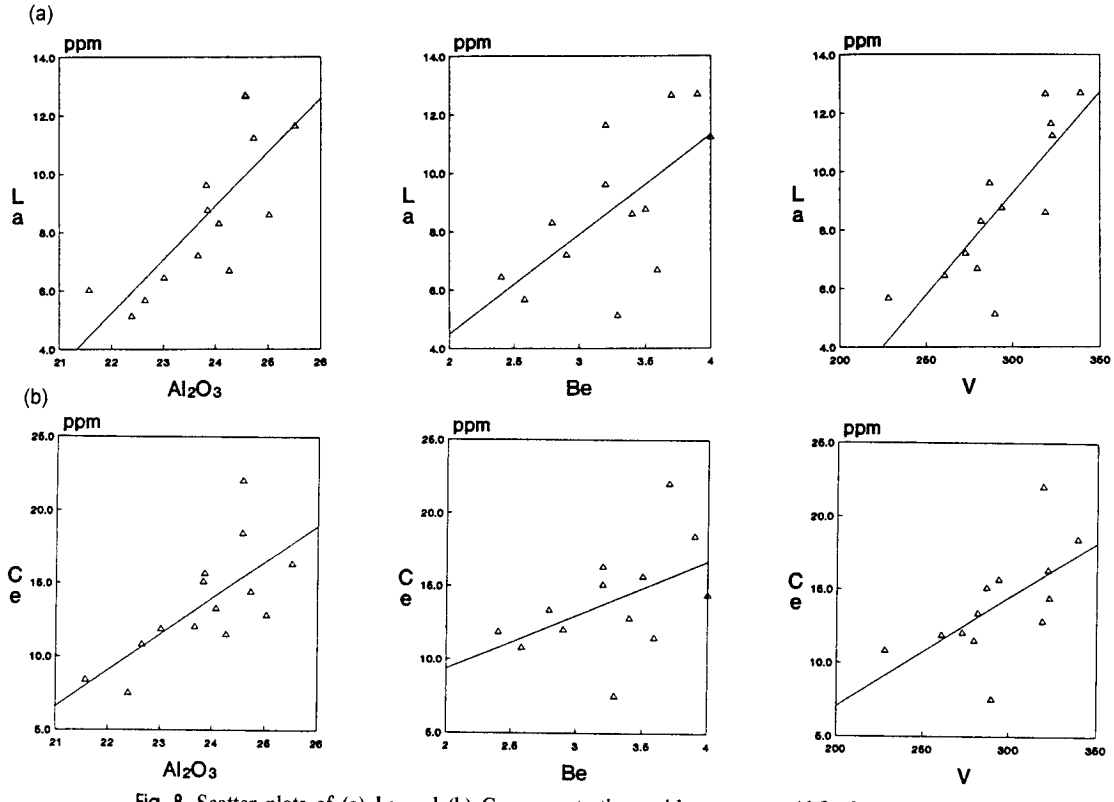

Fig. 8. Scatter plots of (a) La and (b) Ce concentrations with respect to Al_2O_3, Be and V.

Table 3. Structural formulae of I/S. Reindeer D-27.

Sample depth	Structural formulae
6475	$K_{0.12}Na_{0.62}Ca_{0.03}(Al_{1.63}Mg_{0.22}Fe_{0.16}Ti_{0.02})(Si_{3.35}Al_{0.65})O_{10}(OH)_2$
6872*	$K_{0.23}Na_{0.47}Ca_{0.04}(Al_{1.62}Mg_{0.21}Fe_{0.19}Ti_{0.03})(Si_{3.42}Al_{0.58})O_{10}(OH)_2$
6975	$K_{0.23}Na_{0.48}Ca_{0.05}(Al_{1.55}Mg_{0.22}Fe_{0.25}Ti_{0.02})(Si_{3.39}Al_{0.62})O_{10}(OH)_2$
7270*	$K_{0.25}Na_{0.32}Ca_{0.03}(Al_{1.63}Mg_{0.20}Fe_{0.19}Ti_{0.02})(Si_{3.56}Al_{0.44})O_{10}(OH)_2$
7475	$K_{0.27}Na_{0.44}Ca_{0.06}(Al_{1.60}Mg_{0.21}Fe_{0.22}Ti_{0.02})(Si_{3.36}Al_{0.64})O_{10}(OH)_2$
7825*	$K_{0.29}Na_{0.29}Ca_{0.05}(Al_{1.56}Mg_{0.22}Fe_{0.24}Ti_{0.02})(Si_{3.53}Al_{0.47})O_{10}(OH)_2$
8025	$K_{0.32}Na_{0.43}Ca_{0.06}(Al_{1.60}Mg_{0.21}Fe_{0.21}Ti_{0.02})(Si_{3.33}Al_{0.67})O_{10}(OH)_2$
8375*	$K_{0.34}Na_{0.23}Ca_{0.04}(Al_{1.64}Mg_{0.20}Fe_{0.18}Ti_{0.01})(Si_{3.55}Al_{0.45})O_{10}(OH)_2$
8475	$K_{0.33}Na_{0.44}Ca_{0.06}(Al_{1.60}Mg_{0.20}Fe_{0.22}Ti_{0.02})(Si_{3.30}Al_{0.70})O_{10}(OH)_2$
8915*	$K_{0.41}Na_{0.45}Ca_{0.02}(Al_{1.64}Mg_{0.19}Fe_{0.18}Ti_{0.01})(Si_{3.30}Al_{0.70})O_{10}(OH)_2$
9597*	$K_{0.44}Na_{0.44}Ca_{0.02}(Al_{1.62}Mg_{0.18}Fe_{0.20}Ti_{0.01})(Si_{3.26}Al_{0.74})O_{10}(OH)_2$

Sample depth-median depth for drill-cutting samples. * - cores.

because it did not show a trend or correlation with depth and other elements. Ga was dispensed as an octahedral element because of its chemical affinity to Al, though it did not show a relationship to depth, stratigraphy and other elements. Sc, Zn and Zr can be distributed either in interlayer or octahedral sites. However, octahedral sites were chosen, because concentrations of these elements, as for other structural elements, were significantly different between Tertiary and Cretaceous intervals and/or changed systematically with depth. The decrease of Sc, Zn and Zr with depth is probably related to diagenesis, i.e. illitization of I/S (see further discussion below).

REE are expected to occupy interlayer sites because of their large ionic size. Concentrations of REE, especially light REE, increase with depth. They show relatively strong correlations to Be and V which may substitute for tetrahedral Al. The covariance of REE with Be and V is probably due to the valency increase caused by V^{5+} which could be partly counter-balanced by Be^{2+} and, in turn, the local valency deficiency caused by Be could be compensated by high-charge interlayer cations such as REE (+3). Therefore, the increase in concentrations of REE with depth is probably real, although they are considered extremely immobile. In the Gulf Coast, a similar increase in REE concentrations was observed (Chaudhuri and Cullers, 1979); however, it was interpreted as a provenance effect. In the Beaufort-Mackenzie Basin, the increase in REE concentrations is gradual over a depth range of 1km (Fig. 7), corresponding to the interval for which mineralogical analysis also established a linear increase in I-content of I/S from 55 to 78 %I. Therefore, the depth trend for the REE is attributed convincingly to diagenesis, rather than to provenance.

The behavior of structural elements is related to layer-charge development. It appears that octahedral

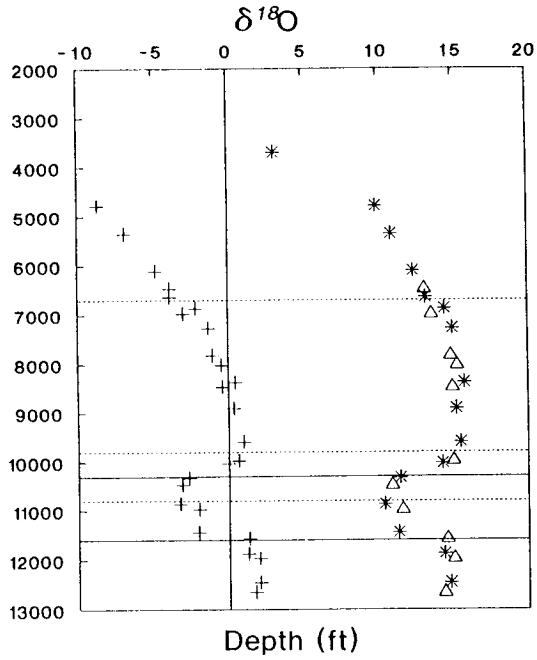

Fig. 9. Depth plot of $\delta^{18}O$ values of I/S and calculated isotopic compositions of pore water according to Savin and Lee (1988). All values in SMOW. For I/S : *; cores, Δ; drill cuttings: pore water +. Solid lines represent discontinuities in oxygen isotope trends. Dashed lines represent the same mineralogical divisions as in Fig. 3 (Note that a 8350ft line is not shown).

sheets release elements such as Mg, Ti, Sc, Zn and Zr that differ in valency and/or ionic size from Al. The release of octahedral elements would decrease the overall layer-charge (see Fig. 10). Fe and transition elements belonging to Groups VI and VIII (Cr, Co and Ni) do not show a statistically significant variation with depth. These elements are di- and trivalent in six-fold coordi-

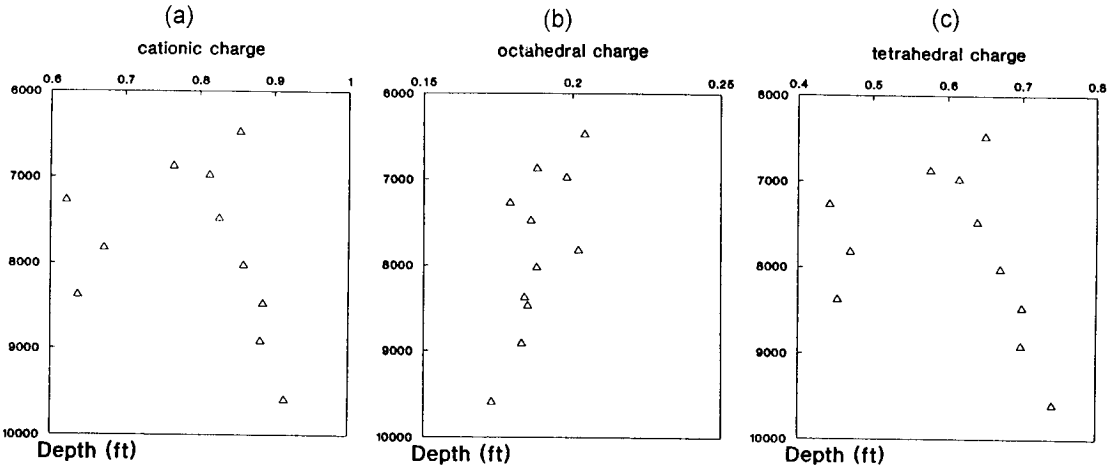

Fig. 10. Plots of (a) cationic, (b) octahedral and (c) tetrahedral charges with depth. For data, see Table 3.

nation. They may better fit in octahedral sites than other elements in terms of valency and ionic size. The increase in Be, V and Al_2O_3 is related to layer-charge development in tetrahedral sheets. To counter the charge increase caused by addition of these tetrahedral elements, Si should be released. However, the trend is obscured by the presence of kaolinite as mentioned previously.

The curves for K_2O and Rb show a close correspondence to the mineralogical trends based on I/S varieties. Concentrations of K_2O increase linearly between 6700 and 9800ft (.1%/1000ft) where the increase in the proportion of I-layers is also linear (~10 %I/1000ft). The lack of regularity in the interval of random I/S is probably due to the occurrence of K and Rb in exchangeable interlayer positions. The depth interval of lower K_2O and Rb concentrations coincides with that of lower I-contents between 9800 and 10800ft (2987~3292m). Concentrations of K_2O and Rb are relatively uniform at about 5% and 160ppm, respectively, in the Cretaceous section where I-contents stay at about 86 %I.

The cationic charge of I/S increases with depth while the tetrahedral charge increases and the octahedral charge decreases (Fig. 10). The overall changes in geochemistry and layer charges are related to illitization of I/S. If a stochastic model applies to I/S minerals, then the layer formulae would be obtained by extrapolating formula composition (Table 3) to 0 and 100 %I, respectively (Fig. 11), and the sum of [%I·(I-layer formula)] and [%S·(S-layer formula)] would approximate the individual structural formulae, and thus chemistry. The smectite layers would have the formula $[Al_{1.57}Fe_{.19}Mg_{.31}Ti_{.07}][Si_{3.84}Al_{.16}]O_{10}(OH)_2$, and the illite layers $[Al_{1.84}Mg_{.16}][Si_{3.33}Al_{.67}]O_{10}(OH)_2$. The resulting layer-formulae are similar to structural formulae for natural smectite and illite minerals.

Oxygen Isotopes

The relatively low $\delta^{18}O$ values are due to ^{18}O-depleted surface water in the high latitudes resulting from the global fractionation of atmospheric, and thus meteoric waters ("Rayleigh effect").

The increase in $\delta^{18}O$ values with depth is very unusual, because the burial increase in temperature and I-contents of I/S would shift the isotopic composition of I/S towards the lower values of pore waters. In the Gulf Coast and elsewhere, $\delta^{18}O$ values of I/S decrease with depth (e.g. Yeh and Savin, 1977). Mathematical models predict that the $\delta^{18}O$ of I/S in isotopic equilibrium with pore water would decrease with increasing burial depth (Suchecki and Land, 1983). However, if the variations in $\delta^{18}O$ values of pore water ($d\delta^{18}O_{pore\ water}$) exceed those due to thermal fractionation ($d\Delta_{I/S\text{-}water}$), different profiles of $\delta^{18}O$ for I/S would result (Fig. 12). If $d\delta^{18}O_{pore\ water} = -d\Delta_{I/S\text{-}water}$, $\delta^{18}O_{I/S}$ will be constant. If $d\delta^{18}O_{pore\ water} > -d\Delta_{I/S\text{-}water}$, $\delta^{18}O_{I/S}$ will decrease with depth. If $d\delta^{18}O_{pore\ water} > -d\Delta_{I/S\text{-}water}$, $\delta^{18}O_{I/S}$ will increase with depth.

The isotopic composition of pore water (see Fig. 9) was calculated according to Savin and Lee (1988):

$1000\ln\alpha_{I/S\text{-}water} = (2.58 + 0.19 \times I) \times 10^6 T^{-2} - 4.19$

where I=fraction of illite-layers which varies between 0.0 and 1.0 (Table 4).

The current geothermal gradient (.6℃/100ft; GEOTECH ENGINEERING, 1983) was assumed to correspond to the downhole temperature gradient at the time whenthe I/S reaction occurred. About 60℃ appeared to be the threshold temperature for active illitization in the Beaufort-Mackenzie Basin (Ko, 1992). This required that

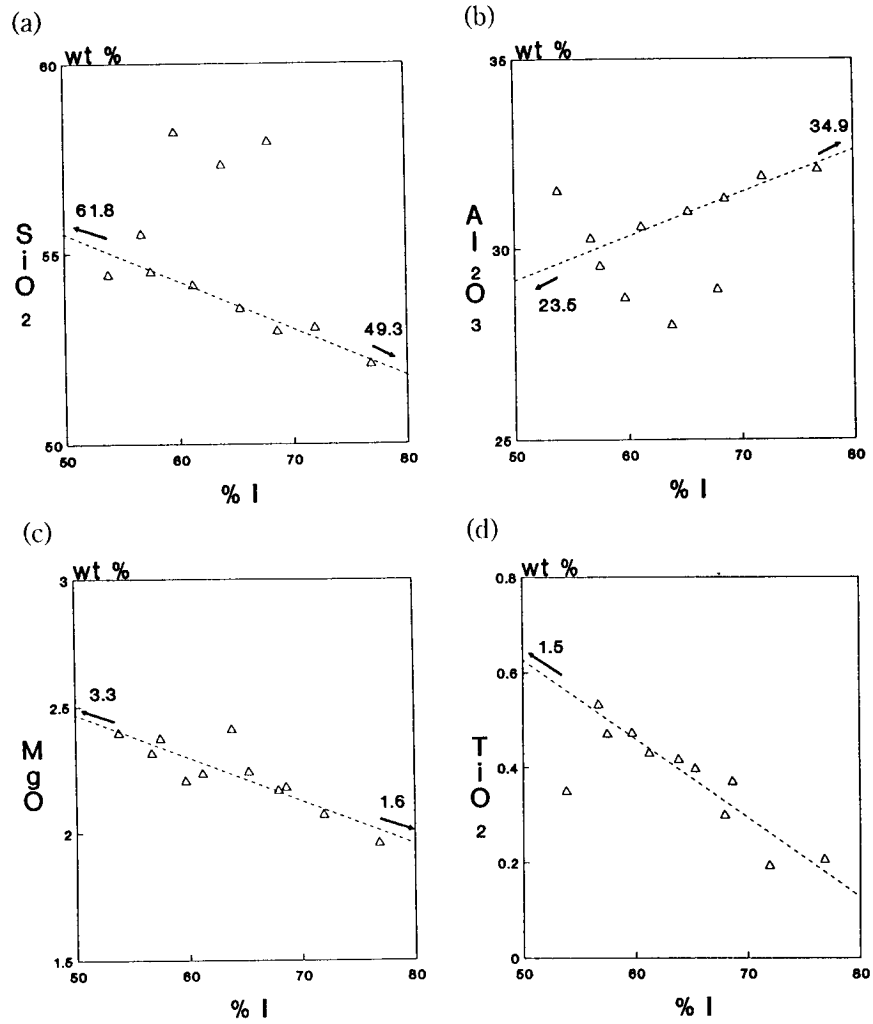

Fig. 11. Plot of (a) SiO_2, (b) Al_2O_3, (c) MgO and (d) TiO_2 concentrations in a formula unit with respect to I-contents. Concentrations of these elements were calculated from the structural formulae in Table 3 and normalized to 100%. Numbers represent extrapolated values to 0 and 100 %I.

the observed I/S compositions were obtained at temperatures about 30℃ higher than, or at depth about 5000ft deeper than at present, which appear to be reasonable estimates conforming to the stratigraphy and the burial history based on basinal trends of I/S diagenesis (Ko, 1992).

The isotopic trends of the pore water suggest that at least two, but possibly as many as four water-masses, each having different isotopic evolution paths, might have existed (Fig. 13a). A single curve could accommodate isotopic compositions other than those between 10329 and 11443ft (3148~3488m) [Fig. 13b]. The regression of isotopic compositions of pore water above 9975ft (3040m) suggests that the pore water might have evolved from water having an original O-isotopic composition of as low as −30‰ (Fig. 13b). The value suggests that the original water was probably meteoric water (−27‰ in the region at present; Longstaffe's personal data).

A discontinuity may exist at about 6700ft (2042m) where the increase in $\delta^{18}O$ of I/S as well as pore water has slowed (Fig. 13a). Pore water below 6700ft might have evolved from water having an original isotopic composition higher than that of the water above. However, at this depth no significant change in stratigraphy and facies is observed. The depth corresponds to the top

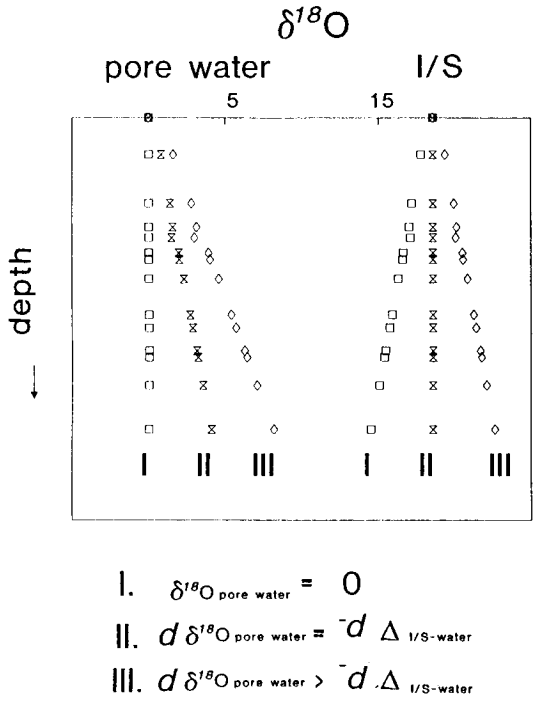

Fig. 12. Models depicting variable oxygen isotopic trends of I/S resulting from variations in $\delta^{18}O$ of pore water. The relative depth and $\Delta_{I/S\text{-water}}$ values are taken from Reindeer D-27 data.

of the interval where ordering of I/S took place. Note that the extrapolation of $\delta^{18}O$ values for ordered I/S and pore water, in general, does not produce the starting isotopic compositions (e.g. Whitney and Northrop, 1988, Fig. 8). Instead, the isotopic trend of ordered I/S intersects the line of random I/S similar to the trends shown in Fig. 13a. Ordering involves large-scale mass transfer, because it requires re-sequencing of randomly arranged I- and S-layers into an orderly form. A full-scale dissolution of I/S may occur at the time of ordering. Thus, ordering might result in complete isotopic resetting of I/S. The subsequent isotopic trend could be related to $\delta^{18}O$ values of I/S and pore water at the time of resetting, however, not to the original composition. Whitney and Northrop(1988) reported a 100% exchange of oxygen with pore water at the transition from random to ordered I/S, compared to partial exchange in reactions of random I/S (up to 65%). Therefore, pore waters above and below 6700ft (2042m) could have evolved from the same water (Fig. 13b). The apparent discontinuity at 6700ft may have resulted from isotopic resetting of I/S at the transition from random to ordered I/S. The gentler slope in the interval of ordered I/S is probably due to

Table 4. Oxygen isotopic composition of I/S and calculated $\delta^{18}O$ of pore water using I/S-water fractionation factors according to Savin and Lee (1988). *- cores. **- projected %I for samples without mineralogical data on the I/S trend curve (see Fig. 2). $\delta^{18}O$ of pore water at 3700ft is not calculated because $\delta^{18}O$ plots out of the trend suggesting I/S may not be in equilibrium with pore water.

Sample depth	$\delta^{18}O_{I/S}$	$\delta^{18}O$ water	Temperature, K	%I	$\Delta_{I/S\text{-water}}$
3700*	3.10	-	325.35	45	19.38
4782*	9.86	−8.67	331.84	40	18.55
5355*	10.89	−6.86	335.28	60	17.75
6113*	12.36	−4.80	339.83	60	17.16
6475	13.12	−3.87	342.00	54**	16.99
6641*	13.17	−3.89	343.00	42	17.06
6872*	14.44	−2.16	344.38	60	16.60
6975	13.57	−2.99	345.00	58**	16.56
7270*	14.96	−1.31	346.77	63	16.27
7825	14.84	−1.06	350.10	62**	15.90
8025	15.25	−0.46	351.30	65	15.71
8375*	15.72	0.45	353.40	79	15.27
8475	14.94	−0.41	354.00	69**	15.35
8915*	15.19	0.35	356.64	84	14.84
9597*	15.46	0.99	360.73	80	14.47
9975	14.98	0.64	363.00	73**	14.34
10028*	14.25	−0.04	363.32	74	14.29
10329*	11.41	−2.67	365.12	76	14.08
10475	10.86	−3.13	366.00	76**	13.99
10867*	10.36	−3.26	368.35	86**	13.62
10975	11.56	−2.00	369.00	86**	13.56
11443*	11.27	−2.05	371.81	84	13.32
11575	14.54	1.32	372.60	86**	13.22
11884*	14.33	1.26	374.45	84	13.07
11975	14.99	2.00	375.00	86**	12.99
12462*	14.75	2.02	377.92	86	12.73
12655	14.36	1.73	379.08	86	12.63

the slowness of the reaction compared to that of random I/S (Ko, 1992). In general, the increase in I-content was fast and showed a parabolic trend with respect to depth in the interval of random I/S, whereas it was slow and linear in the range of ordered I/S in the Beaufort-Mackenzie Basin.

The low $\delta^{18}O$ values between 10329 and 11443ft (3148~3488m) are puzzling. The depth range spans across Tertiary and Cretaceous (Albian) sections, and mineralogically R1- and R>1-ordered I/S intervals (Fig. 2). The depth range overlaps, however, does not coincide with the interval of low I-contents and corresponding geochemical compositions (9800~10800ft; 2987~3292 m), implying that the rearrangement of structural oxygen may have taken place independently of chemical and mineralogical changes in I/S.

The coincidence of the base of the isotopically light interval with the top of the geopressure zone (11600ft; 3536m) suggests that the isotopic composition is pro-

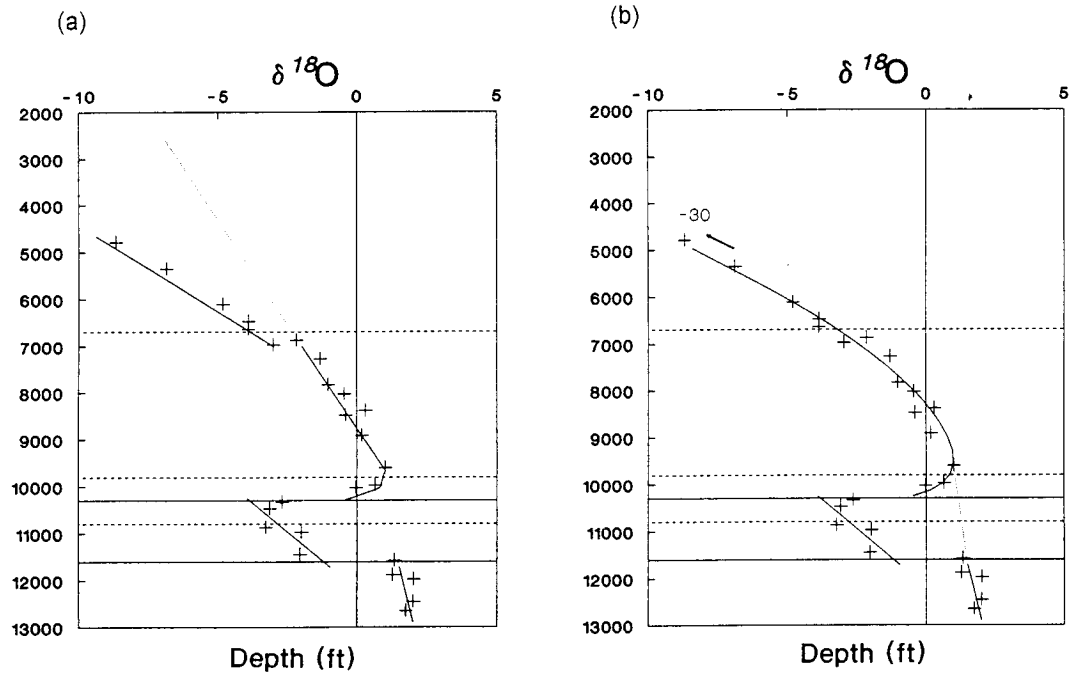

Fig. 13. Interpretation of the isotopic composition of pore water. (a) Individual trends, (b) Single curve with a low band of $\delta^{18}O$. Inflection at about 10000ft is probably due to mixing.

bably related to the hydraulic regime. The inflection of $\delta^{18}O$ to lower values at about 10000ft (3048m) indicates that mixing of water may have taken place. However, the narrowness of the mixing zone suggests that the water in a compartment ~500ft (457 m) thick was effectively isolated from the waters above and below. The geopressured water below 11600ft (3536m) is probably an independent water-mass that had no connection with the major water in the Tertiary section, though the isotopic trend appears to continue after the gap of the anomalous zone to the Tertiary above (Fig. 13b).

The relative timing of emplacement, origin and nature of the isotopically light water-mass in the stratigraphic section encompassing the Tertiary and the Cretaceous (Albian) cannot be determined from the data available. Nevertheless, mineralogy and geochemistry of I/S in the interval provide some clues. Cretaceous I/S from the interval does not show significant differences in composition and chemistry from that below 11600ft (3536m), whereas I/S from the Tertiary section is characterized by relatively low I-content and K_2O concentrations compared to that above 9800ft (2987m). The water chemistry may be related to retarded illitization in the Tertiary section. I/S in the Cretaceous section (10800ft-T. D.; 3292 m-T.D.) had been illitized prior to the emplacement of this isotopically and chemically different water. High $\delta^{18}O$ values of two samples from the lowered I-content and K_2O concentration interval (9975, 10028) may have resulted from later introduction of isotopically heavy water from above.

The isotopically light water might have had a composition which inhibits the illitization process (cf. Roberson and Lahann, 1981), or the relatively closed system hampered the efficient supply of ions essential for the reaction progress. Cannibalization or the internal source was probably insufficient to keep up the pace with the open system above.

CONCLUSIONS

The geochemical trends mirror the I/S mineralogical trend established in the Reindeer D-27 well, Beaufort-Mackenzie Basin. The behavior and concentrations of elements can be related to I/S composition that varied systematically with depth (Fig. 2). I/S in the Beaufort-Mackenzie Basin appears to consist of layers having the formulae of $[Al_{1.57}Fe_{.19}Mg_{.31}Ti_{.07}][Si_{3.84}Al_{1.16}]O_{10}(OH)_2$ and $[Al_{1.84}Mg_{.16}][Si_{3.33}Al_{.67}]O_{10}(OH)_2$ for smectite- and illite-layers, respectively. The increase in concentrations of K_2O, Rb and REE, the decrease in concentrations of octahedral elements such as Mg, Ti, Sc, Zn and Zr, and the increase in concentrations of tetrahedral elements such as Be and V are attributed to the conversion of S-layers to I-layers with increasing depth. The conver-

sion appears to involve the release of octahedral elements other than Al and probably Fe, Co, Cr and Ni. The presence or excess of ions which do not fit into di-octahedral sites of S-layers probably triggers their conversion to I-layers.

The increase in cationic contents of I/S, especially potassium and Rb, is counter-balanced by the increase in layer charge. The selective sorption of ions with low dehydration energy by high-charge layers would result in the formation of I-layers, and thus cause the increase in K_2O and Rb with depth compared to other interlayer elements (e.g. Na^+, Ca^{2+}) that do not show a systematic trend. The total layer-charge increases while the octahedral charge decreases and the tetrahedral charge increases. In other words, the layer-charge development-reaction involves both octahedral and tetrahedral sheets.

The mobilization of REE appears to occur during illitization. Concentrations of REE, especially La and Ce, increase with depth. This is probably linked to incorporation of ions with high valency (e.g. V^{5+}) in tetrahedral sites. The excess valency due to V is partly counter-balanced by ions with low valency (e.g. Be^{2+}) and, in turn, the local valency deficiency caused by Be^{2+} could be compensated by high-charge interlayer cations such as REE (+3).

The behavior of the anion, i.e. oxygen, suggests that pore water may have played an important role in illitization. $\delta^{18}O$ values of I/S increase with depth, which contrasts to decreasing trends observed in the Gulf Coast and elsewhere. The isotopic composition of I/S depends on temperature, I-contents and the isotopic composition of pore water in equilibrium with the clays. The increase in $\delta^{18}O$ of I/S is only possible, if the increase in $\delta^{18}O$ of pore water was greater than the decrease in fractionation values resulting from increased temperature and I-contents with increasing burial depth.

Calculated $\delta^{18}O$ values of pore water in equilibrium with I/S for the Reindeer D-27 well suggest that the original water was probably meteoric water. The stratification of pore water was postulated from the presence of the isotopically light interval, about 450m thick. The depth range of the isotopically light zone overlaps, however, does not coincide with that of low I-contents and corresponding geochemical compositions, suggesting the isotopic re-equilibration. Oxygens may have been exchanged independently of mineralogical and geochemical reactions.

ACKNOWLEDGEMENTS

This paper is part of the first author's Ph.D. thesis. Financial assistance through Strategic and Operating grants from the Natural Sciences and Engineering Research Council of Canada, from the Petroleum Research Fund administered by the American Chemical Society, and Amoco Oil Inc. Canada Petroleum Co. is gratefully acknowledged. J.K. thanks Drs. J. Dixon (Institute of-Sedimentary and Petroleum Geology, Calgary), W. Petruk (CANMET, Ottawa), K. Govindajaru (C.R.P.G., Vandoeuvre, France), Ms. Celine Doule (Department of Medical Sciences, McGill Univ.), and Mr. Paul Middlestead (Univ. Western Ontario, London) for their help at various stages of his study.

REFERENCES

Altaner S.P. and bethke, C.M. (1988) Interlayer order in illite/smectite. Amer. Mineral., v. 73, p. 766-774.

Aronson, J.L. and Hower, J. (1976) Mechanism of burial metamorphism of argillaceous sediments. 2. Radiogenic argon evidence. Geol. Soc. Amer. Bull., v. 87, p. 738-744.

Chaudhuri, S. and Cullers, R.L. (1979) The distribution of rare-earth elements in deeply buried Gulf Coast sediments. Chem. Geol., v. 24, p. 327-338.

Clauer, N., O'neil, J.R., Bonnot-Cardias, C., and Holtzapffel, T. (1990) Morphological, chemical, and isotopic evidence for an early diagenetic evolution of detrital smectite in marine sediments. Clays Clay Minerals, v. 38, p. 33-46.

Clayton, R.N. and Mayeda, T.K. (1963) The use of bromine pentafluoride in the extraction of oxygen from oxides and silicates for isotopic analysis. Geochim. Cosmochim. Acta., v. 27, p. 43-52.

Cullers, R.L., Chaudhuri, S., Arnold, B., Lee, M., and Wolf, C.W.Jr. (1975) Rare-earth distributions in clay minerals and in the clay-sized fraction of the Lower Permian Havensville and Eskridge shales of Kansas and Oklahoma. Geochim. Cosmochim Acta., v. 39, p. 1691-1703.

Eberl, D.D. and Srodon, J. (1988) Ostwald ripening and interparticle diffraction effects for illite crystals. Amer. Mineral., v. 78, p. 1335-1345.

Eberl, D.D., Srodon, J., Kralik, M. Taylor, B.E. and Peterman, Z.E. (1990) Ostwald ripening of clays and metamorphic minerals. Science, v. 248, p. 474-477.

Foscolos, A.E. and Powell, T.G. (1982) Mineralogical and geochemical transformation of clays during catagenesis and their relation to oil generation. In Facts and Principles of World Petroleum Occurrence (ed. A.D. Miall, ed.), p. 153-172, Can. Soc. Petrol. Geol., Memoir, No. 6.

GEOTECH ENGINEERING (1983) Subsurface temperature data from Arctic wells. Earth Physics Branch, Energy, Mines and Resources, Ottawa, Open File 83-11.

Hitchon, B., Underschultz, J.R., Bachu, S., and Sauveplane, C.M. (1990) Hydrogeology, geopressure and hydrocarbon occurrences, Beaufort- Mackenzie Basin. Bull. Can. Petrol. Geol., v. 38, p. 215-235.

Hower, J., Eslinger, E.V., Hower, M.E., and Perry, E.A. (1976) Mechanism of burial metamorphism of argillaceous sediment: 1. Mineralogical and chemical evidence. Geol. Soc. Amer. Bull., v. 87, p. 725-737.

Inoue, A., Velde, B., Meunier, A. and Touchard, G. (1988) Mechanism of illite formation during smectite-to-illite conversion series by scanning and transmission electron microscopes. Amer. Mineral., v. 73, p. 1325-1334.

Ko, J. (1992) Illite/smectite diagenesis in the Beaufort-Mackenzie Basin, Arctic Canada. Ph.D. thesis, McGill University, Canada

Ko, J. and Hesse, R. (1995) Mineralogy of Illite/smectite mixed-layer clays from the Beaufort-Mackenzie Basin, Arctic Canada. In this issue of Econ. Environ. Geol.

Lee, J.H., Ahn, J.H., and Peacor, D.R. (1985) Textures in layered silicates: Progressive changes through diagenesis and low temperature metamorphism. J. Sediment. Petrol., v. 55, p. 532-540.

Morton, J.P. (1985) Rb-Sr evidence for punctuated illite/smectite diagenesis in the Oligocene Frio Formation, Texas Gulf Coast. Geol. Soc. Amer. Bull., v. 96, p. 114-122.

Nadeau, P.H., Wilson, M.J., McHardy, W.J., and Tait, J.M. (1984) Interstratified clays as fundamental particles. Science, v. 225, p. 923-925.

Ohr, M., Halliday, A.N., and Peacor, D.R. (1991) Sr and Nd isotopic evidence for punctuated clay diagenesis, Texas Gulf Coast. Earth Planet. Sci. Lett., v. 105, p. 110-126.

Perry, E.A. and Hower, J. (1970) Burial diagenesis in the Gulf Coast pelitic sediments. Clays Clay Minerals, v. 18, p. 165-177.

Roberson, H.E. and Lahann, R.W. (1981) Smectite to illite conversion rates: Effects of solution chemistry. Clays Clay Minerals, v. 29, p. 129-135.

Savin, S.M. and Lee, M. (1988) Isotopic studies of phyllosilicates. In Reviews in Mineralogy: Hydrous Phyllosilicates (exclusive of micas) (ed. S.W. Bailey), p. 189-223, Mineral. Soc. Amer.

Suchecki, R.K. and Land, L.S. (1983) Isotope geochemistry of burial metamorphosed volcanogenic sediments, Great Valley sequence, northern California. Geochim. Cosmochim. Acta, v. 47, p. 1487-1499.

Whitney, G. and Northrop, H.R. (1988) Experimental investigation of the smectite to illite reaction: Dual reaction mechanisms and oxygen-isotope systematics. Amer. Mineral., v. 73, p. 77-90.

Yeh, H.W. (1980) D/H ratios and late stage dehydration of shales during burial. Geochim. Cosmochim. Acta, v. 44, p. 341-352.

Yeh, H.W. and Savin, S.M. (1977) Mechanism of burial metamorphism of argillaceous sediments: 3. O-isotope evidence. Geol. Soc. Amer. Bull., v. 88, p. 1321-1330.

Manuscript received 18 July 1995

카나다 보포트-맥켄지 분지의 일라이트/스멕타이트의 원소 지화학 및 산소동위원소 연구

고재홍 · R. Hesse · F.J. Longstaffe

요 약 : 보포트-맥켄지 분지의 리인디어 D-27 시추공 시료에 대한 원소 지화학 및 산소동위원소 연구가 수행되었다. K_2O, Rb, 희토류 원소의 함량 증가, Mg, Ti, Sc, Zn, Zr 등의 팔면체 원소의 감소, Be, V 등의 사면체 원소의 증가는 깊이에 따라 일라이트층의 구성비가 증가하는 일라이트/스멕타이트의 속성경향과 대비된다. 스멕타이트층과 일라이트층의 구조식은 각각 $[Al_{1.57}Fe_{.19}Mg_{.31}Ti_{.07}][Si_{3.84}Al_{1.16}]O_{10}(OH)_2$와 $[Al_{1.84}Mg_{.16}][Si_{3.33}Al_{.67}]O_{10}(OH)_2$로 추정된다. 일라이트/스멕타이트의 속성과 연관하여 희토류원소의 유동이 관찰되었다. 희토류원소, 특히 La와 Ce,의 깊이에 따른 함량 증가는 높은 전하가를 갖는 사면체 원소 (V^{5-})의 유입과 관련이 있다. V^{5+}에 의한 잉여 전하는 부분적으로 낮은 전하가를 갖는 Be^{2+}에 의하여 상쇄되며, 또한 Be^{2+}에 의하여 발생하는 지엽적인 전하 불균형은 층간 이온으로는 높은 전하가 (+3)를 갖는 희토류 원소에 의하여 해소된다. 일라이트/스멕타이트의 $\delta^{18}O$가 (SMOW)는 2.91~15.72‰의 범위를 보이며, 걸프연안 등의 일라이트/스멕타이트와는 달리 깊이에 따라 증가한다. 일라이트/스멕타이트의 $\delta^{18}O$가의 증가는 공극수의 $\delta^{18}O$ 증가도가 깊이에 따라 증가하는 온도로 인한 동위원소 분별작용정수 ($\Delta_{I/S\text{-}water}$)의 감소도보다 크기 때문이다. 일라이트/스멕타이트와 평형인 공극수의 $\delta^{18}O$가의 계산결과는 공극수의 근원이 지표수임을 지시한다. 중간 깊이에서 낮은 $\delta^{18}O$가를 보이는 450m 두께의 구간은 공극수가 층상화되어 있음을 의미한다. 그러나 이 깊이 구간이 낮은 일라이트층 구성비와 낮은 K_2O 함량을 보이는 구간과 일치하지 않는 것으로 볼때 동위원소 교환 반응과 광물학적, 지화학적 반응은 서로 독립적으로 일어나는 것으로 해석된다.